

Kinetic and thermodynamic studies on Methylene Blue biosorption by Algerian Olive Stone

K. Batouche*, M. Chikhi, F. Balaska, A. Abbaz

Department of process engineering, Environmental Process Engineering Laboratory (LIPE),
University of Salah Boubnider Constantine 3 – 25000 Constantine, Algeria

*Corresponding author: batouche.khaled@gmail.com ; Tel.: +213 799577297 ; Fax: +21300 00 00

ARTICLE INFO

Article History:

Received : 30/03/2020

Accepted : 22/11/2020

Key Words:

Biosorption;
Olive stone;
Methylene blue;
Kinetic;
Isotherm;
thermodynamic.

ABSTRACT/RESUME

Abstract: Equilibrium adsorption isotherm for the removal of basic dye Methylene Blue (MB) from aqueous solution using olive stone (OS) has been investigated. Equilibrium data were mathematically modelled using the Langmuir, Freundlich, Dubinin-Radushkevich and Temkin adsorption models to describe the equilibrium isotherms and isotherm constants were determined. The results indicate the potential use of the adsorbent to remove MB from the aqueous solution. Maximum adsorption capacity of 2.6 mg.g^{-1} was reached at equilibrium. The Temkin isotherm was found to better fit the correlation coefficient of the experimental data ($R^2 > 0.97$). Pseudo-first-order, pseudo-second-order, Elovich and intraparticle diffusion models were used to study the kinetic data. The results showed that the intraparticle diffusion model was the best one with $R^2=1$ followed by the pseudo-second-order kinetic model. Characteristics of adsorption were determined as spontaneous for $\Delta G^\circ \leq -3.4 \text{ kJ.mol}^{-1}$ and endothermic for ΔH° value of 2.8 kJ.mol^{-1} . The findings obtained suggest that olive stones are a desirable candidate as low-cost biomaterial for extracting simple dye MB from aqueous solutions.

I. Introduction

As understanding that the methylene blue can be used in various fields, including coloring paper, temporary hair coloring, dyeing cotton and wool [1,2]. While vast volumes of dye polluted wastewater are emitted annually resulting in an immediate danger to human safety and the environment [3,4]. MB does not apply to the list of the most harmful contaminants, but rapid exposure in humans induces challenging respiration, increased heart rate, nausea, vomiting, diarrhea, jaundice, quadriplegia, and tissue necrosis[2,5]. The presence of these colors in obtaining water bodies is unwelcome, because they cut off sunlight and may autotrophic organism photosynthetic activities[6]. The concern is that such colors are durable and non-biodegradable [7]; dyes are engineered to retain pigment on various surfaces and to withstand water, soap and oxidizing agents[8]. The removal of dyes from industrial effluents is thus a difficult problem

and refining dye-removal methods is important. The poor performance, high cost and, in certain situations, the development of toxic by-products make certain physical and chemical solutions such as filtration, coagulation, photocatalytic degradation and advanced oxidation processes inefficient and costly to operate[9]. Biosorption has been shown to be an effective and inexpensive solution, especially when using biowaste and agricultural by-products as biosorption. The quest for low-cost and locally accessible waste materials for dyes biosorption continues and has been intensified extensively [3,11,12,13,14]. Of this purpose, biomaterials may be used for other products such as Cr(VI), Cd(II), Cr(III) AND Pb(II) [15,16] as low cost sorbents. Olive stone biomass, a by-product of the olive oil industry, has also been used as an adsorbent for iron, which has a great capacity for extracting metal ions from effluent not just from the olive oil industry but also from other polluted wastewater across a broad spectrum of concentrations [17]. A further economic

and environmental alternative is the use of raw olive stones as biosorbents. This provides an incentive for the olive processing industry to make good use of the immense amounts of olive; Algeria's olive grown region was about 188,923 ha in 2011. Total table olive output in 2011 was estimated at 192,785 tons [18,19], especially in Algeria's rural areas such as Mila and TiziOuzou. Upon referring to its coloring operations, the biomass upon-product of olive stone has been shown to be effective for the biosorption of Methylene Blue dyes[20], as well as for methylene blue biosorption on olive stone[21].

Methylene blue (MB) was chosen as a simple dye model to test the adsorption potential from olive stone aqueous solutions, a green agro-waste and without economic benefit. The main objective of this study is to investigate the biosorption equilibrium kinetic experimental data; thermodynamic parameters and the factors controlling of the olive stone adsorption process on MB were calculated and discussed in this present work.

II. Materials and methods

II.1. Adsorbent preparation

Olive stones were used as natural help in this analysis, and were collected from the Mila area. The purification and washing process is focused on several measures from the raw material, which includes impurities on its outer surface that must be eliminated by washing; thus, washing and drying are indispensable; afterward, the dried material is milled using a traditional and electrical grinder; after this stage, it must be washed 4 times with purified water each time with one-liter under agitation of 20min; we also place it in a 24 hours drying oven at 105°C and finalize the last sieving stage (0.315 mm) with the powder form used in the current job.

II.2. Adsorbate preparation

Methylene Blue (cationic dye), taken as a pattern of toxins, is used without proper purification. Dissolving the proportions of the pigment in distilled water strengthens the solutions. For distilled water, solutions were formulated for dyes with a concentration of $C_0 = 10 \text{ mg/L}$. Successive dilutions are performed to create curves of the absorbance concentration = f (concentrations of methylene blue). The chemical structure of MB is shown in Fig.1.

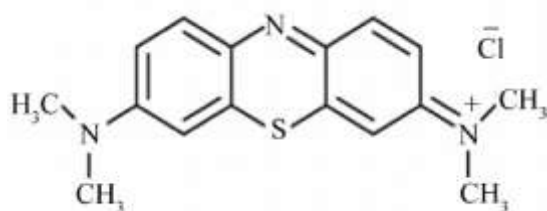


Figure 1. Chemical structure of methylene blue

II.3 Adsorption experiments

Briefly, the calculation of the adsorption potential included the addition of an equal mass of olive stones in a series of 25ml volume beakers in which MB solutions were inserted (mixed concentration between 1 and 10 mg / L). For a moment, for proper solid-liquid isolation, the samples are put into a centrifuge for 15 min, then the liquid phase is spectrophotometrically evaluated at a wavelength of 664 nm.

II.4. Kinetic studies

Kinetic tests for dye biosorption were performed at 50 mL glass beaker with 25 mL of 10 mg.L^{-1} dye concentration comprising 0.15 g of biosorbent at 298 K with stirring temperature. Samples were collected at various time intervals (0-60 min), evaluated for concentrations of unremoved pigment, as mentioned above. At equilibrium, biosorption capacity, q_e (mg.g^{-1}), was determined using Eq. (1):

$$q_e = \left(\frac{C_i - C_f}{X} \right) \quad (1)$$

Where C_i and C_f are the concentrations of original and final dyes (mg.L^{-1}), and X is the concentration of biosorbents in solution (g.L^{-1}).

Among a variety of kinetic models, pseudo-first-order [22], pseudo-second-order [23], Elovich and intraparticle diffusion [24] models were chosen to find an appropriate model for better representation of kinetic biosorption.

The linear form of the equation for the pseudo-first-order can be represented as Eq. (2):

$$\ln(q_e - q_t) = \ln q_e - K_1 t \quad (2)$$

Where q_e and q_t are the sums of the dye adsorbed by biomass (mg.L^{-1}) at equilibrium and after period t , and K_1 is the pseudo-first-order constant (min^{-1}), respectively.

The pseudo-second-order model can be written in linear form as Eq(3):

$$\frac{t}{q_t} = \frac{1}{K_2 q_e^2} + \frac{1}{q_e} \quad (3)$$

Where q_e and q_t are biomass adsorbed dye numbers at equilibrium and period t (mg.g^{-1}), and K_2 is the pseudo-second-order constant ($\text{g.mg}^{-1}.\text{min}^{-1}$), respectively. The statistical method for the concept of intraparticle diffusion may be called an Eq (4):

$$q_t = K_i t^{\frac{1}{2}} + C \quad (4)$$

Where K_i ($\text{mg}\cdot\text{g}^{-1}\cdot\text{min}^{-1/2}$) and C represents constant of intraparticle diffusion rate and intercept, respectively.

The Elovich equation is a rate function based on the widely stated in adsorption kinetic studies as the following function Eq.(5) [25,26,27]:

$$\frac{dq_t}{dt} = \alpha \exp(-\beta q_t) \quad (5)$$

Where α is the initial adsorption rate ($\text{mg}\cdot\text{g}^{-1}\cdot\text{min}^{-1}$), and β is the desorption constant ($\text{g}\cdot\text{mg}^{-1}$) relevant to the degree of the surface coverage and chemisorptive activation capacity.

Equation (5) is simplified by assuming $\alpha \beta \gg t$ and applying boundary conditions $q_t = 0$ at $t = 0$, and $q_t = q_t$ at $t = t$ becomes:

$$q_t = \frac{1}{\beta} \ln(\alpha\beta) + \frac{1}{\beta} \ln t \quad (6)$$

II.5. Isotherm studies

Under the aforementioned conditions, equilibrium tests were performed with various initial dye concentrations ($1-10 \text{ mg}\cdot\text{L}^{-1}$), utilizing 0.15g of biomass at 298 K for 60 min . The most commonly known isothermic equations were used for the models Langmuir, Freundlich, Temkin and Dubinin-Radushkevich.

The Langmuir isotherm [28] claims a monolayer adsorption of a substantial number of similar locations onto a solid base. The Langmuir isotherm model is expressed as mentioned in Eq (7)

$$q_e = \frac{q_m b C_e}{1 + b C_e} \quad (7)$$

The linear form of Langmuir isotherm is presented as:

$$\frac{1}{q_e} = \frac{1}{q_m} + \frac{1}{b q_m} \times \frac{1}{C_e} \quad (8)$$

Where q_e ($\text{mg}\cdot\text{g}^{-1}$) is the adsorption capacity at equilibrium for monolayer adsorption, C_e is the concentration of sorbate in equilibrium solution ($\text{mg}\cdot\text{L}^{-1}$) and b ($\text{L}\cdot\text{mg}^{-1}$) is the constant of Langmuir related to free energy or net enthalpy.

The isotherm adsorption model of the Freundlich [29], which allows for a heterogeneous multilayer adsorption, is commonly used to explain the isothermic biosorption of the dyes. It is stated by exponential Eq (9):

$$q_e = K_f C_e^{\frac{1}{n}} \quad (9)$$

Freundlich isotherm linear form is defined by the following equation:

$$\ln q_e = \ln K_f + \frac{1}{n} \ln C_e \quad (10)$$

K_f is the Freundlich constant ($(\text{mg}\cdot\text{g}^{-1})(\text{L}\cdot\text{mg}^{-1})^{1/n}$), and n is the biosorption rate.

The model Dubinin and Radushkevich(D-R) [30] were chosen for calculating the apparent free biosorption energy. Eq.(11) defines the linear shape of the D-R isothermic equation:

$$\ln q_e = \ln Q_m - k_d \varepsilon^2 \quad (11)$$

Where q_e is the quantity of adsorbed dye on the biomass ($\text{mg}\cdot\text{g}^{-1}$), Q_m is the maximum biosorption power ($\text{mg}\cdot\text{g}^{-1}$); k_d is the coefficient of activity ($\text{mol}^2\cdot\text{J}^{-2}$) referring to the mean energy of biosorption, and ε is the Polanyi potential, determined through Eq. (12):

$$\varepsilon = RT \ln \left(1 + \frac{1}{C_e} \right) \quad (12)$$

Where T (K) is the absolute temperature and R is the gas constant ($8.314 \text{ J}\cdot\text{mol}^{-1}\cdot\text{K}^{-1}$).

Using the activity coefficient, the mean biosorption energy ($\text{kJ}\cdot\text{mol}^{-1}$), which is an indicator of the process involved in biosorption, can be calculated according to Eq. (13):

$$E = \frac{1}{\sqrt{2k_d}} \quad (13)$$

The adsorption cycle is chemically regulated when the E value is within the range from 8 to $16 \text{ kJ}\cdot\text{mol}^{-1}$ and when E is $< 8 \text{ kJ}\cdot\text{mol}^{-1}$ it defined by a physical mechanic.

Finally, the experimental results were modeled by Temkinisotherm [31] in order to explain some indirect adsorbent/adsorbent interactions on the isothermic dye biosorption. The model Temkin is given by Eq. (14):

$$q_e = B \ln a_T + B \ln C_e \quad (14)$$

where

$$B = \frac{RT}{b_T} \quad (15)$$

Where a_T ($L.g^{-1}$) the binding constant of equilibrium compared to the maximal binding energy and b_T ($kJ.mol^{-1}$) is the Temkin constant correlated with the adsorption heat.

II.6. Thermodynamic studies

Biosorption of methylene blue was tested at various temperatures (298, 303, 308, 313 and 318 K) to examine the thermodynamic parameters such as the normal shifts in Gibbs free energy (ΔG°), enthalpy (ΔH°) and entropy (ΔS°). Biosorption free energy change ($J.mol^{-1}$) can be determined by the Van't Hoff equation [32] as Eq.(16):

$$\Delta G^0 = -RT \ln K_d \tag{16}$$

Where $K_d(L.g^{-1})$ is the coefficient of distribution and is equivalent to q_e / C_e .

Free energy transition can be expressed at a constant temperature as Eq.(17):

$$\Delta G^0 = \Delta H^0 - T\Delta S^0 \tag{17}$$

III. Results and discussions

III.1. Adsorption Isotherm study

The adsorption isotherm plays an important role in determining the maximum capacity and for identifying the type of adsorption. It is obtained by the graphic representation of the adsorption capacity q_e as a function of the dye concentration C_e , the adsorption isotherm of MB on the adsorbent OS is presented in Fig. 2.

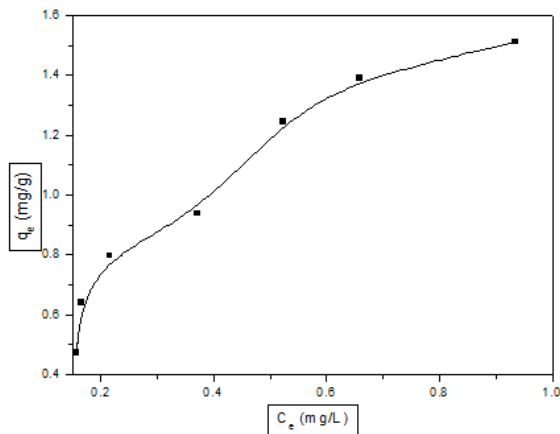


Figure 2. Adsorption isotherm for the removal of MB onto OS

III.1.1. Langmuir isotherm

Fig.3 depicts the plot of $1/q_e$ vs. $1/C_e$. The values of Langmuir constants q_m and b were computed from the slope and intercept of the plot, and are given in Table 1 along with correlation coefficient (R^2). From the data of this research work, the adsorption

capacity q_m was determined by linear Langmuir equation to be $2.6 mg.g^{-1}$ of MB on OS, b of $1.6 L.mg^{-1}$, the R^2 value of 0.9066 proving that the Langmuir Isotherm model is less applicable for the removal of MB on OS. The characteristic parameter of Langmuir isotherm can be illustrated in terms of dimensionless equilibrium parameter R_L , also known as separation factor, defined by Weber and Chakkravorti [33]:

$$R_L = \frac{1}{1 + bC_0} \tag{18}$$

The R_L value indicates the type of isotherm as follows

Value of R_L	Type of isotherm
$R_L > 1$	Unfavourable
$R_L = 1$	Linear
$0 < R_L < 1$	Favourable
$R_L = 0$	irreversible

Where C_0 is the initial concentration of the sorbate. The value R_L offers an indication of the isotherm type and the nature of the adsorption process. The value of R_L is 0.05 demonstrates that the nature of adsorption is favourable. The maximum monolayer adsorption capacities of the Langmuir isotherm of OS for the removal of MB was compared with other adsorbents reported in the literature. It is clear from Table.2 that OS's adsorption capacity was comparable to the capacities previously reported.

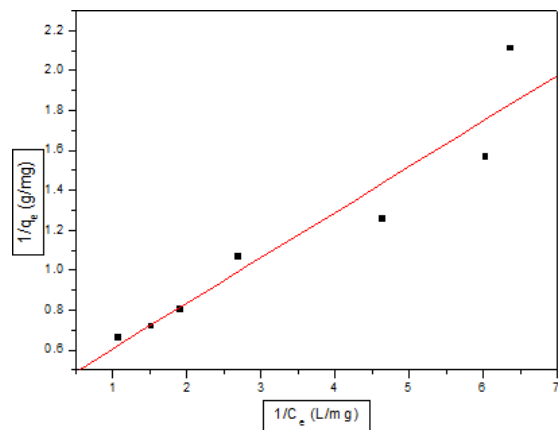


Figure 3. Langmuir isotherm for the adsorption of MB onto OS

III.1.2 Freundlich isotherm

The plot of $\ln q_e$ vs $\ln C_e$ of the Freundlich equation and from the resulting figure K_f can be evaluated from the intercept of the plot as shown in Fig.4. The correlation coefficients, $R_2 = 0.9313$, implies that the experimental data fitted well to the Freundlich model. From Table.1, the magnitudes of K_f and n indicate easy adsorption of MB with strong adsorptive capacity for the OS sorbent. The value of n was 1.6 which suggests that the adsorption occurred as a chemical process ($n > 1$) [34].

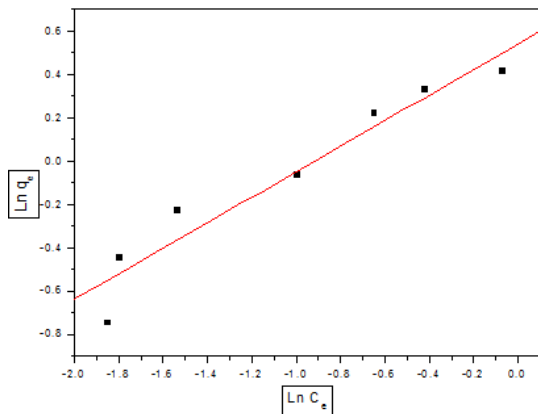


Figure 4. Freundlich isotherm model for the adsorption of MB onto OS

III.1.3. Dubinin-Radushkevich isotherm

The plot of $\ln q_e$ vs ε^2 is shown in Fig.5. Table.1 shows the constant obtained for D – R isotherms. The mean adsorption energy E provides details on the chemical and physical nature of adsorption [35]. It was found to be $3244.4 \text{ kJ.mol}^{-1}$, which confirms that the adsorption reaction is chemical.

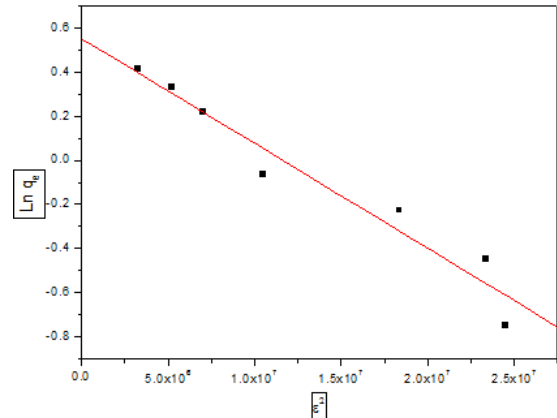


Figure 5. Dubinin-Radushkevich isotherm model for the adsorption of MB onto OS

III.1.4 Temkin isotherm

The plot of q_e vs $\ln C_e$ is illustrated in Fig.6. The isotherm constants were determined from the slope and intercept. The linear plot for Temkin adsorption isotherm fits quite well with correlation coefficient R^2 of 0.97. Thus, the adsorption of MB on OS is a chemisorption process [36]. The positive value of constant b_T shows that the adsorption process is endothermic [37].

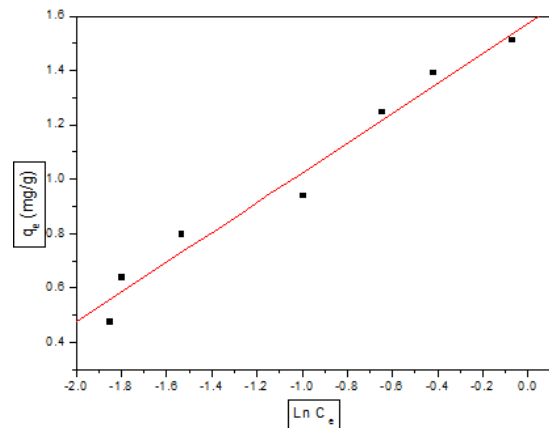


Figure 6. Temkin isotherm for the adsorption of MB onto OS

Table 1. Equilibrium model parameters for adsorption of MB onto OS adsorbent

Isotherm model	Parameter	Parameter Value
Langmuir	$q_m(\text{mg}\cdot\text{g}^{-1})$	2.6
	$b(\text{L}\cdot\text{mg}^{-1})$	1.6
	R_L	0.05
	R^2	0.9066
Freundlich	n	1.6
	$K_f((\text{mg}\cdot\text{g}^{-1})(\text{L}\cdot\text{mg}^{-1})^{1/n})$	1.7
	R^2	0,9313
Temkin	$a_T(\text{L}\cdot\text{g}^{-1})$	17.4
	B	0.5
	$b_T(\text{kJ}\cdot\text{mol}^{-1})$	4493.6
	R^2	0.9720
Dubinin-Radushkevich	$Q_m(\text{mg}\cdot\text{g}^{-1})$	1.7
	$k_d(\text{mol}^2\cdot\text{kJ}^{-2})$	$4.7\cdot 10^{-8}$
	$E(\text{kJ}\cdot\text{mol}^{-1})$	3244.4
	R^2	0.9509

Table 2. Comparison of OS with other sorbents for the removal of MB

Adsorbent	Adsorption capacity $q_m(\text{mg}\cdot\text{g}^{-1})$	pH	C	References
Wheat shells	16.56	2-4	100-400 mg/l	[5]
Neem (<i>Azadirachta indica</i>) leaf powder	3.67	2-10	2-10 g/l	[38]
Spent coffee grounds	18.73	5	0-250 mg/l	[39]
Naturel zeolite	19.94	7.5	30-250 mg/l	[40]
Glass wool	2.24	8.3	0-100 mg/l	[41]
Clay	6.3	7	0-1 mg/l	[42]
Calcined raw kaolin	7.59	4-10	0-0.5 mg/l	[43]
Living biomass	1.17	4-10	0-50 mg/l	[44]
Wheat straw	2.23	8	1.4-14 mg/l	[45]
Chrome sludge	0.51	3.5-9	5-40 mg/l	[46]
Fly ash	1.10	5	0-1 mmol/l	[47]
Egg shell and agg shell membrane	0.80	-	1-10 mg/l	[48]

acid-bound iron oxide magnetic nanoparticles	0.199	9	0.5-8 mg/l	[49]
Olive stone	2.6	3-10	3-10 mg/l	This work

III. 2. Adsorption kinetics

The biosorption of MB dye onto OS as a function of contact time is shown in Fig.7. Biosorption studies were carried out for 60 min. It was observed that the amount of MB dye increased with time and the equilibrium were established in 15min. The initial fast uptake is probably due to the high initial MB concentration and empty dye binding sites on OS. Whereas the rate of biosorption decreases due to the saturation of dye binding sites.

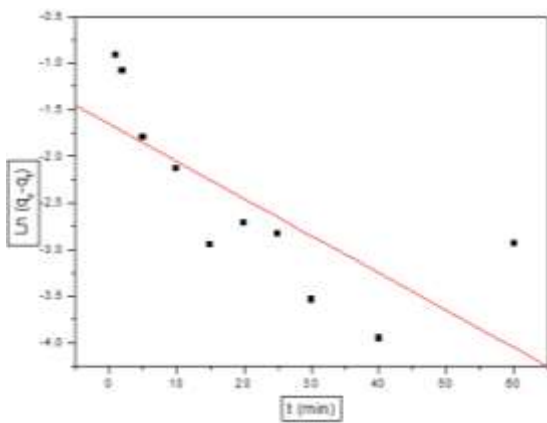


Figure 7. Effect of contact time on adsorption of MB onto OS

III.2.1. Pseudo-first-order

The plot of $\ln(q_e - q_t)$ vs. t is illustrated in Fig.8. The $\ln(q_e - q_t)$ values were correlated linearly with t . K_1 's plot value was calculated from plot slope (Table.3). For certain cases, Lagergren's first-order model does not fit well with the entire contact time range and is generally applicable over the initial stage of the adsorption processes [50].

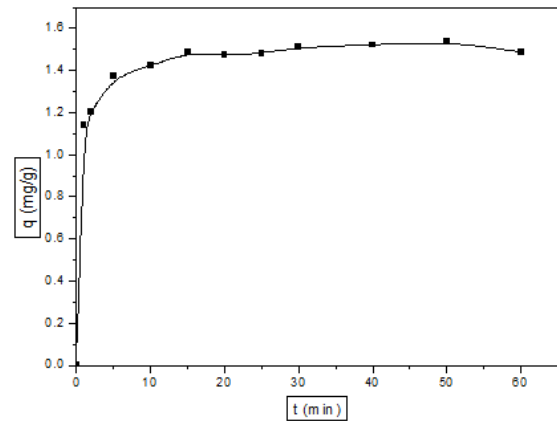


Figure 8. Pseudo-first-order kinetic for MB adsorption onto OS

III.2.2. Pseudo-second-order

The slope and intercept of plot of t/q_t vs t were used to calculate the second-order rate constant K_2 (Fig.9). The values of equilibrium rate constant (K_2) are presented in Table.3. The correlation coefficient of the examined data was found very high ($R^2 \geq 0.999$). This shows that the model can be applied for the entire adsorption process and confirms that the sorption of direct MB on OS follows the pseudo-second-order kinetic model.

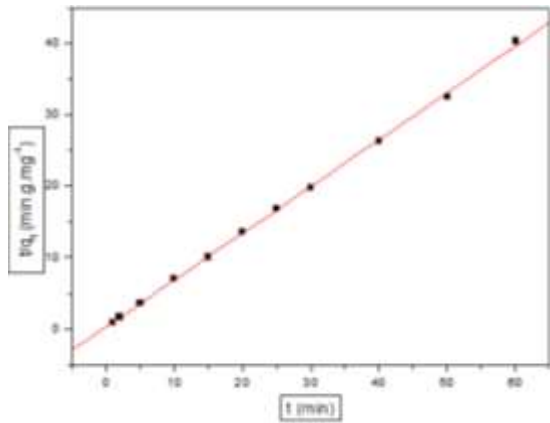


Figure 9. Pseudo-second-order kinetic for MB adsorption onto OS

III.2.3. Elovich

The Plot of q_t vs. $\ln t$ is shown in Fig.10, the constant β was calculated from the slope of the straight line and the constant α was calculated from the intercept. The Elovich equation did not match the experimental data very well. The table.3 includes information on the parameters obtained by this kinetic model as well as the correlation coefficients (average $R^2 = 0.9150$).

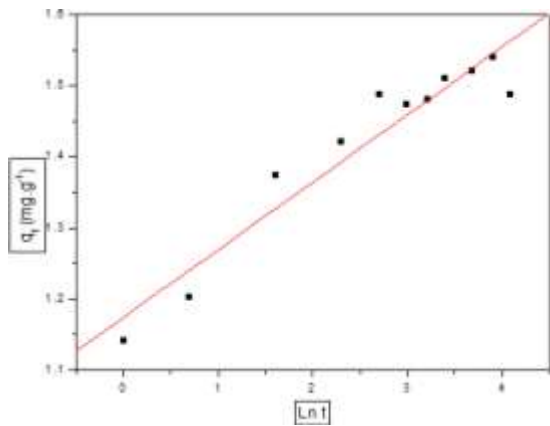


Figure 10. Elovich model plot for the adsorption of MB onto OS

III.2.4. Intra-particle diffusion

The intraparticle diffusion rate constants values are illustrated in Table.3. Fig.11 revealed that the plot of qt vs. $t_{1/2}$ was multi-linear, indicating that more than one step is involved in the adsorption process [51]. It is observed that there are three linear portions, which elucidate the adsorption stages: external mass

transfer at initial period followed by intraparticle diffusion of MB on OS; adsorption on the interior sites. In the initial phase, from the slope of the graph it is clear, that bulk diffusion becomes the ratecontrolling step. The diffusion of MB ionsthrough the solution to the external surface of the sorbent happens here. In the second phase, gradual sorption stage, diffusion of the solute into mesopores occurs. The rate of removal of solute from the bulk depends on the size of the sorbate molecule, the concentration of the sorbate, diffusion coefficient of sorbate in the bulk of the solution and the pore size distribution of the sorbent [52]. The third portion of the plot suggests biosorption into the micropores of the sorbent.

The diffusion coefficient, D_i , for the intraparticle transport of MB into the adsorbent particles has been calculated by Eq.19 [53]

$$D_i = \frac{0.3r^2}{t_{1/2}} \quad (19)$$

Where $t_{1/2}$ is the time of half adsorption (s), r is the adsorbent particle radius (cm), and D_i is the diffusion coefficient in $\text{cm}^2.\text{s}^{-1}$. In the current study, D_i is found to be in the range of $10^{-10}\text{cm}^2.\text{s}^{-1}$. The diffusivity coefficient for all chemisorption systems should be 10^{-5} to $10^{-13}\text{cm}^2.\text{s}^{-1}$. The value of the coefficient of pore diffusion D_i of MB is given in Table.3 and the present study follows the chemisorption systembut it is not the only limiting step of the phenomenon because the linear plots do not pass through the origine.

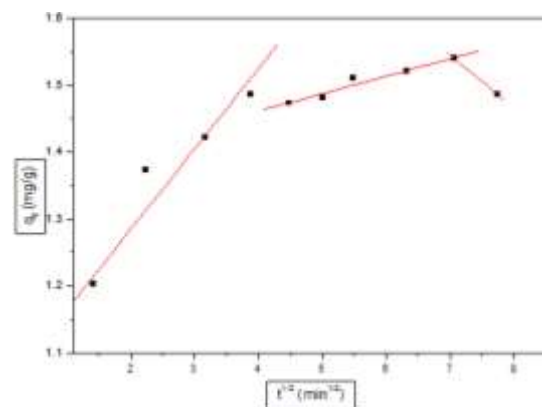


Figure 11. Intraparticle diffusion model for MB adsorption onto OS

Table 3. Kinetic parameters for the removal of MB

Kinetic models	Parameter	Parameter Value
Pseudo-first-order	q_e (mg.g ⁻¹)	0.2
	K_1 (min ⁻¹)	0.04
	R^2	0.57
Pseudo-second-order	q_e (mg.g ⁻¹)	1.5
	K_2 (g.mg ⁻¹ .min ⁻¹)	1.4
	R^2	0.9993
Elovich	$q_e = 1/\beta$ (mg/g)	0.9
	α (mg / g.min)	2.3
	β (g/mg)	1.1
	R^2	0.9150
Intra-particle diffusion	K_{i1} (mg.g ⁻¹ .min ^{-1/2})	0.1
	C_1 (mg.g ⁻¹)	1.04
	R_1^2	0.9435
	K_{i2} (mg.g ⁻¹ .min ^{-1/2})	0.03
	C_2 (mg.g ⁻¹)	1.3
	R_2^2	0.8737
	K_{i3} (mg.g ⁻¹ .min ^{-1/2})	-0.1
	C_3 (mg.g ⁻¹)	2.1
	R_3^2	1
	D_i (cm ² .s ⁻¹)	$7.3.10^{-10}$

IV. Thermodynamic study

The values of ΔH° and ΔS° were calculated from the slope and intercept of plot between $\ln K_d$ versus $1/T$ for initial MB concentration of 10 mg/l as shown in Fig.12. The calculated values of ΔH° , ΔS° and ΔG° are listed in Table.4. The ΔH° value obtained is 2.8 in kJ/mol. The positive sign indicates that the process is endothermic in nature [54,55,56]. This behavior might be due to the increase of diffusion rate of adsorbate across the external boundary layer and internal pores of adsorbents [57,58]. ΔS° value obtained is positive 21 J/mol.K suggesting that during adsorption at the solid–liquid interface, the degree of freedom increased [58]. Besides, the positive value indicates the randomness at solid–liquid interface reflecting the affinity of adsorbate towards the adsorbent [59, 60]. The negative value of ΔG° indicates that the adsorption process is spontaneous.

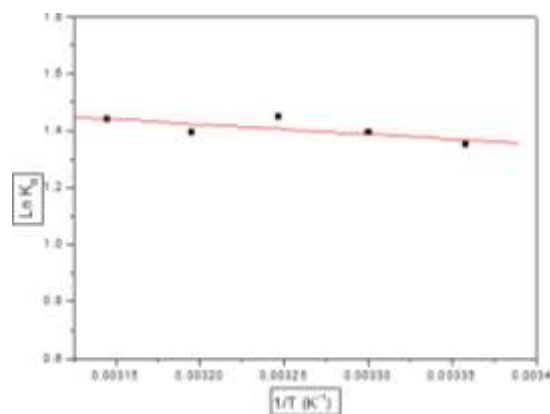


Figure 12. Plot of $\ln K_d$ vs. $1/T$ for estimation of thermodynamic parameters

Table 4. Thermodynamic parameters values for the adsorption of MB onto OS

Temperature °K	ΔG° (kJ/mol)	ΔH° (kJ/mol)	ΔS° (J/mol.k)
298	-3.4	2.8	21
303	-3.5		
308	-3.6		
313	-3.7		
318	-3.8		

IV. Conclusion

The equilibrium, kinetic and biosorption thermodynamic study with olive stone was conducted for the biosorptive removal of MB. Of the four isotherm models applied, Langmuir, Freundlich Dubinin-Radushkevich and Temkin, Temkin isotherm was found to best fit the experimental data as indicating from the high values of the correlation coefficients ($R^2 > 0.97$).

The closeness of the correlation coefficient to unity would indicate a perfect fit. The adsorption system study show favourable adsorption of MB as indicated from the low value of RL ($0 < R_L < 1$).

Kinetic data were tested using the pseudo- first-order, pseudo-second-order Intraparticle diffusion and Elovich equation. The kinetics of the adsorption process was found to follow the both of Intraparticle diffusion and pseudo-second-order kinetic models, suggesting that the adsorption process was controlled by chemisorption. Biosorption mechanism and the intraparticle diffusion model suggest that more than one mechanism controls the rate-limiting step.

The thermodynamic investigation shows that the negative value of ΔG° and positive sign of ΔH° indicate that the adsorption is endothermic and spontaneous in nature.

The adsorption of MB onto OS presented in this paper make this adsorbent a promising one in the field of adsorption for the removal of synthetic dye in wastewater treatment.

V. References

- Kumar, K.; Vasanth, V.; Ramamurthi, Sivanesan, S. Modeling the mechanism involved during the sorption of methylene blue onto fly ash." *Journal of colloid and interface science* 284.1 (2005) 14-21.
- Banat, F.; Al-Asheh, S.; Al-Ahmad, R.; Bni-Khalid, F. Bench-scale and packed bed sorption of methylene blue using treated olive pomace and charcoal. *Bioresource technology* 98.16 (2007) 3017-3025.
- Cao, J. S.; Lin, J. X.; Fang, F.; Zhang, M. T.; Hu, Z. R. A new adsorbent by modifying walnut shell for the removal of anionic dye: kinetic and thermodynamic studies. *Bioresource technology* 163 (2014) 199-205.
- Semeraro, P.; Rizzi, V.; Fini, P.; Matera, S.; Cosma, P.; Franco, E.; ... Fortea, I. Interaction between industrial textile dyes and cyclodextrins. *Dyes and Pigments* 119 (2015) 84-94.
- Bulut, Y.; Aydın, H. A kinetics and thermodynamics study of methylene blue adsorption on wheat shells. *Desalination* 194.1-3 (2006) 259-267.
- Albadarin, A. B.; Mo, J.; Glocheux, Y.; Allen, S.; Walker, G.; Mangwandi, C. Preliminary investigation of mixed adsorbents for the removal of copper and methylene blue from aqueous solutions. *Chemical engineering journal* 255 (2014) 525-534.
- Ari, A. G.; Celik, S. Biosorption potential of Orange G dye by modified Pyracanthacoccinea: Batch and dynamic flow system applications. *Chemical engineering journal* 226 (2013) 263-270.
- Khataee, A. R.; Vafaei, F.; Jannatkah, M. Biosorption of three textile dyes from contaminated water by filamentous green algal *Spirogyra* sp.: Kinetic, isotherm and thermodynamic studies. *International Biodeterioration & Biodegradation* 83 (2013) 33-40.
- Kabbout, Rana, and Samir Taha. Biodecolorization of textile dye effluent by biosorption on fungal biomass materials. *Physics Procedia* 55 (2014): 437-444.
- Albadarin, A. B.; Mangwandi, C.; Walker, G. M.; Allen, S. J.; Ahmad, M. N. Biosorption characteristics of sawdust for the removal of Cd (II) ions: mechanism and thermodynamic studies. *Chem. Eng. Trans* 24 (2011) 1297-1302.
- Abdolali, A.; Guo, W. S.; Ngo, H. H.; Chen, S. S.; Nguyen, N. C.; Tung, K. L. Typical lignocellulosic wastes and by-products for biosorption process in water and wastewater treatment: a critical review. *Bioresourcetchnology* 160 (2014) 57-66.
- Guerrero-Coronilla, I.; Morales-Barrera, L.; Cristiani-Urbina, E. Kinetic, isotherm and thermodynamic studies of amaranth dye biosorption from aqueous solution onto water hyacinth leaves. *Journal of environmental management* 152 (2015) 99-108.
- Magriotis, Z. M.; Vieira, S. S.; Saczk, A. A.; Santos, N. A.; Stradiotto, N. R. Removal of dyes by lignocellulose adsorbents originating from biodiesel production. *Journal of Environmental Chemical Engineering* 2.4 (2014) 2199-2210.
- Wang, M. X.; Zhang, Q. L.; Yao, S. J. A novel biosorbent formed of marine-derived *Penicillium janthinellum* mycelial pellets for removing dyes from dye-containing wastewater. *Chemical Engineering Journal* 259 (2015) 837-844.
- Fiol, N.; Villaescusa, I.; Martinez, M.; Miralles, N.; Poch, J.; Serarols, J. Biosorption of Cr (VI) using low cost sorbents. *Environmental Chemistry Letters* 1.2 (2003) 135-139.
- Calero, M.; Hernández, F.; Blázquez, G.; Martín-Lara, M. A.; Tenorio, G. Biosorption kinetics of Cd (II), Cr (III) and Pb (II) in aqueous solutions by olive stone. *Brazilian Journal of Chemical Engineering* 26.2 (2009) 265-273.
- Hodaifa, G.; Ochando-Pulido, J. M.; Alami, S. B. D.; Rodríguez-Vives, S.; Martínez-Ferez, A. Kinetic and thermodynamic parameters of iron adsorption onto

- olive stones. *Industrial crops and products* 49 (2013) 526-534.
18. Soufi, O. ; Romero, C.; Louaileche, H. Ortho-diphenol profile and antioxidant activity of Algerian black olive cultivars: Effect of dry salting process. *Food chemistry* 157 (2014) 504-510.
 19. ITAFV. (2011). Technical Institute of Fruit and Vine Arboriculture. Table olives statistics 2011. Study Department General Direction (Algiers)
 20. Albadarin, A. B., Mangwandi, C. Mechanisms of Alizarin Red S and Methylene blue biosorption onto olive stone by-product: Isotherm study in single and binary systems. *Journal of environmental management* 164 (2015) 86-93.
 21. Trujillo, M. C.; Martín-Lara, M. A.; Albadarin, A. B., Mangwandi, C.; Calero, M. Simultaneous biosorption of methylene blue and trivalent chromium onto olive stone. *Desalination and Water Treatment* 57.37 (2016) 17400-17410.
 22. Lagergren, S. About the theory of so-called adsorption of soluble substances, *Kungliga Svenska Vetenskapsakademiens Handlingar* 24 (1898) 1–39, as cited by HC Trivedi, M. Patel, RD Patel, Adsorption of cellulose triacetate on calcium silicate. *J. Eur. Polym.* 9 (1973) 525-531.
 23. Ho, Y. S.; McKay, G. Pseudo-second order model for sorption processes. *Process biochemistry* 34.5 (1999) 451-465.
 24. Weber, W. J.; Morris, J. C. Kinetics of adsorption on carbon from solution. *Journal of the sanitary engineering division* 89.2 (1963) 31-60.
 25. Zeldowitsch, J. Über den mechanismus der katalytischenoxydation von CO an MnO₂. *Actaphysicochim. URSS* 1 (1934): 364-449.
 26. Chien, S. H.; Clayton, W. R. Application of Elovich equation to the kinetics of phosphate release and sorption in soils 1. *Soil Science Society of America Journal* 44.2 (1980) 265-268.
 27. Sparks, D. L. Kinetics of reaction in pure and mixed systems. *Soil physical chemistry* 44 (1986) 265-268.
 28. Langmuir, I. The adsorption of gases on plane surfaces of glass, mica and platinum. *Journal of the American Chemical society* 40.9 (1918) 1361-1403.
 29. Freundlich, H. M. F. Over the adsorption in solution. *J. Phys. Chem* 57.385471 (1906) 1100-1107.
 30. Dubinin, M. M. The equation of the characteristic curve of activated charcoal. *Dokl.Akad.Nauk. SSSR* 55 (1947) 327-329
 31. Temkin, M. I. Kinetics of ammonia synthesis on promoted iron catalysts. *Actaphysicochim. URSS* 12 (1940) 327-356.
 32. Tan, C. Y.; Li, M.; Lin, Y. M.; Lu, X. Q.; Chen, Z. L. Biosorption of Basic Orange from aqueous solution onto dried *A. filicoides* biomass: Equilibrium, kinetic and FTIR studies. *Desalination* 266.1-3 (2011) 56-62.
 33. Weber, T. W.; Chakravorty, R. K. Pore and solid diffusion models for fixed-bed adsorbers. *AICHE Journal* 20.2 (1974) 228-238.
 34. Ghasemi, M.; Mashhadi, S.; Asif, M., Tyagi, I.; Agarwal, S.; Gupta, V. K. Microwave-assisted synthesis of tetraethylenepentamine functionalized activated carbon with high adsorption capacity for Malachite green dye. *Journal of Molecular Liquids* 213 (2016) 317-325.
 35. Rieman, W.; Walton, H. F. *Ion exchange in analytical chemistry: international series of monographs in analytical chemistry*. Elsevier (2013).
 36. Biswas, K.; Saha, S. K.; & Ghosh, U. C. Adsorption of fluoride from aqueous solution by a synthetic iron (III) aluminum (III) mixed oxide." *Industrial & Engineering Chemistry Research* 46.16 (2007) 5346-5356.
 37. Ahmad, M. A.; Ahmad, N.; Bello, O. S. Modified durian seed as adsorbent for the removal of methyl red dye from aqueous solutions. *Applied Water Science* 5.4 (2015) 407-423.
 38. Bhattacharyya, K. G.; Sharma, A. Kinetics and thermodynamics of methylene blue adsorption on neem (*Azadirachta indica*) leaf powder. *Dyes and pigments* 65.1 (2005) 51-59.
 39. Franca, A. S.; Oliveira, L. S.; Ferreira, M. E. Kinetics and equilibrium studies of methylene blue adsorption by spent coffee grounds. *Desalination* 249.1 (2009) 267-272.
 40. Han, R.; Zhang, J.; Han, P.; Wang, Y.; Zhao, Z.; Tang, M. Study of equilibrium, kinetic and thermodynamic parameters about methylene blue adsorption onto natural zeolite. *Chemical Engineering Journal* 145.3 (2009) 496-504.
 41. Chakrabarti, S.; Dutta, B. K. On the adsorption and diffusion of methylene blue in glass fibers. *Journal of colloid and interface science* 286.2 (2005) 807-811.
 42. Shawabkeh, R. A.; Tutunji, M. F. Experimental study and modeling of basic dye sorption by diatomaceous clay. *Applied Clay Science* 24.1-2 (2003) 111-120.
 43. Ghosh, D.; Bhattacharyya, K. G. Adsorption of methylene blue on kaolinite. *Applied clay science* 20.6 (2002) 295-300.
 44. Fu, Y.; Viraraghavan, T. Removal of a dye from an aqueous solution by the fungus *Aspergillus niger*. *Water Quality Research Journal* 35.1 (2000) 95-111.
 45. Batzias, F.; Sidiras, D.; Schroeder, E.; Weber, C. Simulation of dye adsorption on hydrolyzed wheat straw in batch and fixed-bed systems. *Chemical Engineering Journal* 148.2-3 (2009) 459-472.
 46. Lee, C. K.; Low, K. S.; Chow, S. W. Chrome sludge as an adsorbent for colour removal. *Environmental technology* 17.9 (1996) 1023-1028.
 47. Woolard, C. D.; Strong, J.; Erasmus, C. R. Evaluation of the use of modified coal ash as a potential sorbent for organic waste streams. *Applied Geochemistry* 17.8 (2002) 1159-1164.
 48. Tsai, W. T.; Yang, J. M.; Lai, C. W.; Cheng, Y. H.; Lin, C. C.; Yeh, C. W. Characterization and adsorption properties of eggshells and eggshell membrane. *Bioresource technology* 97.3 (2006) 488-493.
 49. Mak, S. Y.; Chen, D. H. Fast adsorption of methylene blue on polyacrylic acid-bound iron oxide magnetic nanoparticles. *Dyes and pigments* 61.1 (2004) 93-98.
 50. Ahmad, A. A., Hameed, B. H.; Aziz, N. Adsorption of direct dye on palm ash: Kinetic and equilibrium modeling. *Journal of hazardous materials* 141.1 (2007) 70-76.
 51. Annadurai, G.; Juang, R. S.; Lee, D. J. Use of cellulose-based wastes for adsorption of dyes from aqueous solutions. *Journal of hazardous materials* 92.3 (2002) 263-274.
 52. Cheung, W. H.; Szeeto, Y. S.; McKay, G. Intraparticle diffusion processes during acid dye adsorption onto chitosan. *Bioresource technology* 98.15 (2007) 2897-2904.
 53. Sepehr, M.N.; Amrane, A.; Karimaian, K. A.; Zarrabi, M.; Ghaffari, H. R. Potential of waste pumice and surface modified pumice for hexavalent chromium removal: Characterization, equilibrium, thermodynamic and kinetic study. *Journal of the Taiwan Institute of Chemical Engineers* 45.2 (2014) 635-647.
 54. Ahmad, M. A.; Puad, N. A. A.; Bello, O. S. Kinetic, equilibrium and thermodynamic studies of synthetic dye removal using pomegranate peel activated carbon

- prepared by microwave-induced KOH activation. *Water Resources and industry* 6 (2014) 18-35.
55. Ahmed, M. J. Application of agricultural based activated carbons by microwave and conventional activations for basic dye adsorption. *Journal of Environmental Chemical Engineering* 4.1 (2016) 89-99.
 56. Ahmed, M. J. Preparation of activated carbons from date stones by chemical activation method using FeCl₃ and ZnCl₂ as activating agents. *Journal of Engineering* 17.4 (2011) 1007-1022.
 57. Bello, O. S.; Ahmad, M. A.; Ahmad, N. Adsorptive features of banana (*Musa paradisiaca*) stalk-based activated carbon for malachite green dye removal. *Chemistry and Ecology* 28.2 (2012) 153-167.
 58. Bello, O. S.; Fatona, T. A.; Falaye, F. S.; Osuolale, O. M.; Njoku, V. O. Adsorption of eosin dye from aqueous solution using groundnut hull-based activated carbon: kinetic, equilibrium, and thermodynamic studies. *Environmental Engineering Science* 29.3 (2012) 186-194.
 59. Baek, M.H.; Ijagbemi, C.O.; Se-Jin, O.; Kim, D. S. Removal of Malachite Green from aqueous solution using degreased coffee bean. *Journal of hazardous materials* 176.1-3 (2010) 820-828.
 60. Önal, Y.; Akmil-Başar, C.; Eren, D.; Sarıcı-Özdemir, Ç.; Depci, T. Adsorption kinetics of malachite green onto activated carbon prepared from Tunçbilek lignite. *Journal of hazardous materials* 128.2-3 (2006) 150-157.

Please cite this Article as:

Batouche K., Chikhi M., Balaska F., Abbaz A., Kinetic and thermodynamic studies on Methylene Blue biosorption by Algerian Olive Stone, *Algerian J. Env. Sc. Technology*, 7:4 (2021) 2121-2132